

Silicon nanowires to enhance the performance of self-powered near-infrared photodetectors with asymmetrical Schottky contacts

Ahmad I. Nusir, Stephen J. Bauman, Mohammed S. Marie, Joseph B. Herzog, and M. Omar Manasreh

Citation: *Appl. Phys. Lett.* **111**, 171103 (2017);

View online: <https://doi.org/10.1063/1.5001053>

View Table of Contents: <http://aip.scitation.org/toc/apl/111/17>

Published by the [American Institute of Physics](#)

Scilight

Sharp, quick summaries **illuminating**
the latest physics research

Sign up for **FREE!**

AIP
Publishing

Silicon nanowires to enhance the performance of self-powered near-infrared photodetectors with asymmetrical Schottky contacts

Ahmad I. Nusir,^{1,a)} Stephen J. Bauman,² Mohammed S. Marie,² Joseph B. Herzog,³ and M. Omar Manasreh¹

¹Electrical Engineering Department, University of Arkansas, Fayetteville, Arkansas 72701, USA

²Microelectronics-Photonics Graduate Program, University of Arkansas, Fayetteville, Arkansas 72701, USA

³Department of Physics, University of Arkansas, Fayetteville, Arkansas 72701, USA

(Received 21 August 2017; accepted 15 October 2017; published online 26 October 2017)

Silicon nanowires were etched vertically in the channel between asymmetrical interdigital electrodes. The self-powered near-infrared photodetector consists of a planar structure of Au-vertically aligned Si nanowire-Ti. The devices were characterized by measuring the current-voltage characteristics, the external quantum efficiency (EQE), and the spectral response. An enhancement of 32% in the short-circuit current was achieved after applying the Si nanowires. The EQE of the device with Si nanowires consists of a strong peak covering the near-infrared spectral range with a maximum EQE of 10.3% at 965 nm and 0 V. Furthermore, the spectral response measurements showed enhancement and broadening in the spectrum of devices with Si nanowires.

Published by AIP Publishing. <https://doi.org/10.1063/1.5001053>

Silicon nanowires were found to be attractive for various optoelectronic devices due to their interesting optical and electrical properties, which include light trapping, quantum confinement, and efficient charge collection.^{1–3} Several designs were proposed to incorporate Si nanowires into photodetectors, such as metal-insulator-semiconductors,⁴ vertical Schottky junctions,^{5,6} metal-semiconductor-metal,^{7,8} PN and heterojunctions,^{9–11} and single nanowire devices.¹² Additionally, many approaches were employed to enhance the performance of solar cells by utilizing Si nanowires.^{13–17} Enhancement in the power conversion efficiency was obtained due to the higher photocurrent, which is attributed to the strong light absorption in the nanocrystalline structure.^{18–21}

The dynamics of light absorption and the generation of photo-excited carriers are the basis of operation of photodetectors, which involve efficient transport and collection of photo-excited carriers as well. This can be achieved by using two asymmetrical Schottky barriers in contact with the semiconductor, which will create a built-in electric field responsible for collecting the photo-excited carriers without external biasing.²² Moreover, the absorption of light can be enhanced by applying Si nanowires through the utilization of the anti-reflection property exhibited in the nanowires.²³

Vertically aligned Si nanowires can be fabricated by using various etching approaches that are based on metal-assisted wet etching.²⁴ Among them is electroless etching, which has been widely used in fabricating Si nanostructures for its simplicity and low-cost.²⁵ It is a top-down etching approach and based on coating the surface of Si with a noble metal, such as Ag, to catalyze etching of Si under the metal in the presence of HF acid and H₂O₂. On the other hand, the use of less electronegative metals than Si such as Cr can block this catalytic etching and act as a hard mask for metal-assisted wet etching.²⁶ In this article, we report on the enhancement in the photoresponsivity of a self-powered

near-infrared photodetector based on asymmetrical Schottky interdigital electrodes using Si nanowires. The Si nanowires were etched vertically in the channel between planar Au and Ti electrodes placed on an undoped Si substrate. The photoresponsivity of devices with and without the nanowires was extracted by measuring the current-voltage characteristics, external quantum efficiency (EQE), and spectral response.

An undoped Si substrate was used in the fabrication of the devices to enable achieving low dark currents. The structure of the self-powered near-infrared photodetector and the fabrication steps are plotted in Fig. 1. First, Si fingers with a thickness and a width of 3 and 50 μm , respectively, were prepared by wet etching. The wet etchant consists of HF(49%):HNO₃(70%):H₂O with a volume ratio of 6:10:40. Second, Cr (70 nm) was deposited between the Si fingers to protect the areas where the final interdigital electrodes will be deposited. Third, the Si fingers were transformed into nanowires by electroless etching.^{11,25} In this process, the Si sample was coated with Ag nanoparticles by placing it in a solution of 4.8 M of HF and 0.005 M of AgNO₃ under stirring for 1 min and then immersed in an HF etchant for

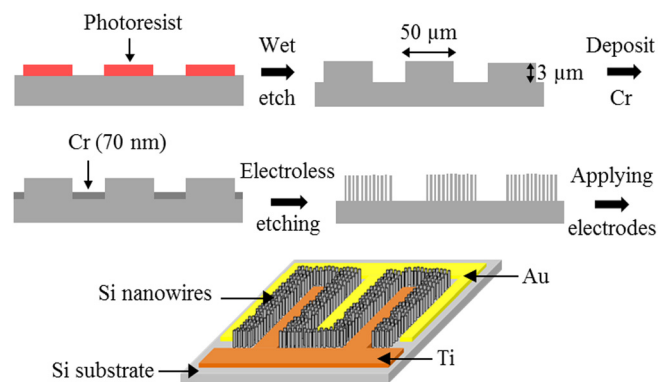


FIG. 1. Fabrication steps of the self-powered near-infrared photodetector based on Si nanowires and a schematic showing the final structure of the device.

^{a)}Author to whom correspondence should be addressed: ainusir@uark.edu

40 min. Finally, the Cr hard mask was removed, and Au and Ti interdigital electrodes (30 nm) were deposited between the Si nanowires by optical photolithography. This involves first depositing a comb-like shape of Au and then the Au thin-film and the Si nanowires were covered with photoresist and Ti was deposited, similar to the procedure presented in previous work.²⁷

Metal deposition was performed using an Angstrom Nexdep e-beam evaporator. Scanning electron microscopy (SEM) imaging was performed using a Nova nanolab-250 at 18 kV. The current-voltage characteristics were measured using a Keithley 4200 SCS. The photocurrent was measured under illumination (360–1800 nm) covering the entire area of the device with a power density of 100 mW/cm². The spectral response was measured using a Bruker IFS 125HR FTIR spectrometer, and the EQE was measured using an Oriel IQE200 spectrometer.

The SEM image of the vertically aligned Si nanowires is shown in Fig. 2(a) with a scale bar of 5 μ m. It was found that the diameters of the grown Si nanowires vary in the range between 89 and 165 nm with an average value of 125 nm. Figure 2(b) shows a cross-sectional SEM image of the Si nanowires, and it shows nanowires with a length of 3 μ m. This length of the nanowires was achieved by setting the etching time in the HF acid to 40 min. These obtained dimensions (diameter and length) agree with a previous report on Si nanowires grown by electroless etching with the same procedure.¹¹

The current density-voltage (J - V) characteristics under dark and illumination conditions of the control device and the device with Si nanowires are plotted together in Fig. 3. The control device is made from Au and Ti interdigital electrodes spaced by a 50 μ m channel and without Si nanowires between the electrodes. The current density in the units of mA/cm² was found by dividing the current by the active area of the device, which is 0.13 cm². The devices had a diode J - V behavior, and under illumination, the curve shifts downwards by the value of light-generated current, which is similar to the J - V curve of a typical solar cell. Under illumination, the control device has an open-circuit voltage of 0.23 V and a short-circuit current density of 11.6 mA/cm². The short-circuit current density increases to 15.3 mA/cm² after adding the Si nanowires inside the channel, which corresponds to an enhancement of 32%.

The EQE spectra in percentage at 0 V bias for both the control device and the device with Si nanowires are plotted in Fig. 4. The control device has a flat EQE spectrum with an

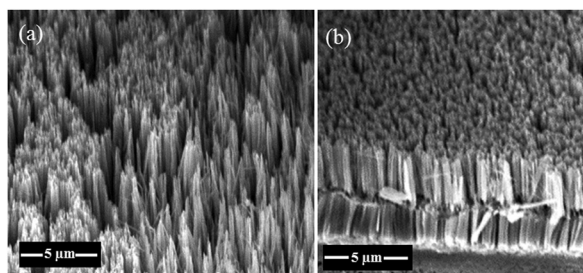


FIG. 2. (a) SEM image of the vertically aligned Si nanowires grown by electroless etching and (b) cross-sectional SEM image of the nanowires.

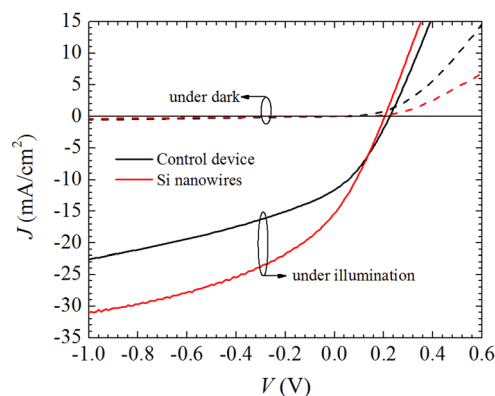


FIG. 3. J - V characteristics of the control device and the device with Si nanowires in dark conditions (dashed lines) and under illuminations (solid lines).

onset at a wavelength of 1200 nm and an average EQE value of 5.4%. Significant enhancement in the EQE in the near-infrared spectral region (800–1200 nm) was achieved after applying the Si nanowires. The EQE spectrum of the Si nanowire device has a peak ranging from the visible to the near-infrared spectral region and with a maximum EQE value of 10.3% at 965 nm. The full width at half maximum (FWHM) of the EQE peak is 450 nm. The steps observed in the EQE spectra at a wavelength of 720 nm are due to the change in the gratings in the Oriel spectrometer.

Further enhancement and broadening were obtained after applying the Si nanowires as shown in the spectral response of the devices in Fig. 5. The spectral response in arbitrary units was measured at 0 V for both the control device and the device with Si nanowires. The spectral response results in Fig. 5 are consistent with the EQE measurements plotted in Fig. 4. With Si nanowires, the spectral response of the device increases rapidly above the band-edge of Si as compared to the control device. The rapid decay in the spectral response of the devices in the higher energy region is due to the response of the quartz beam splitter in the Bruker FTIR spectrometer. While this decay is not observed in the EQE spectra plotted in Fig. 4, since the Oriel spectrometer is a double monochromator and the beam splitter is not required.

It is well known that Si nanowires grown by electroless etching are capable of enhancing the light absorption by

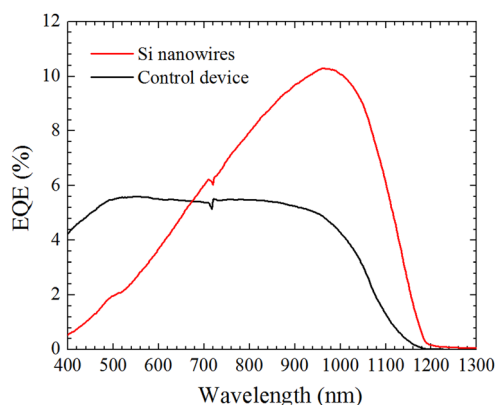


FIG. 4. EQE in percentage at 0 V bias of the control device and the device with Si nanowires.

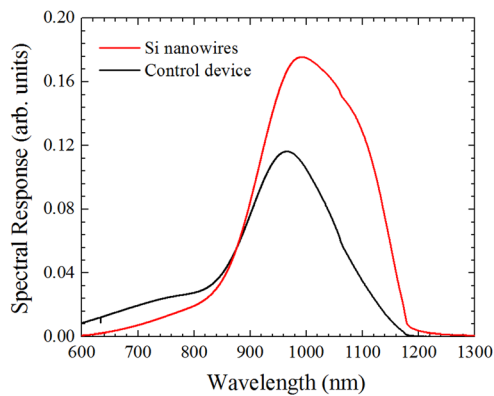


FIG. 5. Spectral response in arbitrary units at 0 V bias of devices with and without the Si nanowires.

suppressing the reflection from the surface.^{25,28} This stronger light absorption is responsible for the enhancement seen in the photoresponsivity of the devices. The reflection from the surface depends on the length of the nanowires and decreases with longer ones.²⁹ Therefore, an increase in the length of the nanowires is expected to further enhance the photoresponsivity of the devices.

The operation at 0 V bias is due to the band bending in Si caused by the asymmetric Schottky barrier heights formed at the Au/Si and Ti/Si interfaces, which are 1.09 and 0.32 eV, respectively.³⁰ This band bending will create a built-in electric field that will separate the photo-excited carriers, generating a photocurrent at 0 V. The Schottky barrier height depends on the difference between the metal work function and the electron affinity of the semiconductor. The increase in the Schottky barrier height will strengthen the built-in electric field and provide an efficient separation of the photo-excited carriers.¹⁷ The formation of the Schottky junction can be confirmed from the obtained diode rectifying behavior, as can be seen in the J - V curves of the devices plotted in Fig. 3.

The peak centered at a wavelength of 965 nm in the EQE spectrum of the device with Si nanowires results from the quantum confinement in the nanowires and is associated with the intrinsic transition above the band-edge of Si.¹² The reduction in the EQE spectrum of the Si nanowire device in the higher energy region (>1.8 eV) can be attributed to the excessive surface recombination of the photo-excited carriers over the surface of the Si nanowires caused by the large surface-to-volume ratio.³¹ This reduction in the high energy region is also exhibited in other photovoltaic devices based on Si nanowires.^{12,15}

The responsivity (R) in the unit of A/W can be extracted from the EQE spectra in Fig. 4 using the following formula: $R(\lambda) = \text{EQE} \cdot \lambda / 1240$, where λ is the wavelength in nm. The maximum responsivity at 0 V of the device with Si nanowires was found to be 0.08 A/W at 965 nm. This responsivity at 0 V is on the same order of the responsivity obtained from other photodetectors with the same planar structure (metal-Si nanowires-metal) and biased at -10 V.^{7,8} Other work reported the vertical structure of ITO-Si nanowire-Al with a responsivity of 0.3 A/W at 800 nm and -2 V,⁶ while in this work, the obtained responsivity at the same wavelength and 0 V bias is 0.05 A/W. Increasing the reverse bias voltage of

the self-powered photodetector will enhance the built-in electric field of the junction and consequently increase the responsivity of the device. Furthermore, the integration of Si nanowires with interdigital electrodes spaced by a shorter channel will further enhance the device performance by increasing the electric field inside the channel.²⁷

In conclusion, we presented a method to enhance the performance of self-powered near-infrared photodetectors using vertically aligned Si nanowires. The Si nanowires were selectively grown in the active area of the device by electroless etching and Cr hard mask. Enhancement in the short-circuit current was achieved due to the stronger light absorption in the Si nanowires. The EQE measurements showed that the device based on Si nanowires can efficiently detect at 0 V in the near-infrared spectral region as compared to the other device without nanowires. The Si nanowires are also capable of enhancing and broadening the spectral response of the devices above the band-edge of Si. This work has demonstrated an approach to design and fabricate optoelectronic devices based on Si nanowires grown by top-down etching. Furthermore, this work has provided a way to utilize the unique optical properties of the Si nanowires in order to improve the performance of devices.

The authors thank Mr. Errol Porter for his assistance in etching the samples and also Dr. Mourad Benamara for his help in the SEM imaging.

- ¹E. Garnett and P. Yang, *Nano Lett.* **10**, 1082 (2010).
- ²L.-B. Luo, L.-H. Zeng, C. Xie, Y.-Q. Yu, F.-X. Liang, C.-Y. Wu, L. Wang, and J.-G. Hu, *Sci. Rep.* **4**, 3914 (2014).
- ³O. H. A. Zoubi, T. M. Said, M. A. Alher, S. E. Ghazaly, and H. Naseem, *Opt. Express* **23**, A767 (2015).
- ⁴J. Bae, H. Kim, X.-M. Zhang, C. H. Dang, Y. Zhang, Y. J. Choi, A. Nurmikko, and Z. L. Wang, *Nanotechnology* **21**, 095502 (2010).
- ⁵P. Servati, A. Colli, S. Hofmann, Y. Q. Fu, P. Beecher, Z. A. K. Durrani, A. C. Ferrari, A. J. Flewitt, J. Robertson, and W. I. Milne, *Physica E* **38**, 64 (2007).
- ⁶L. P. Hackett, M. A. Seyed, M. Fiorentino, and R. G. Beausoleil, *J. Phys. D: Appl. Phys.* **50**, 215105 (2017).
- ⁷M. M. Adachi, K. Wang, F. Chen, and K. S. Karim, *Proc. SPIE* **7622**, 76224M (2010).
- ⁸E. Mulazimoglu, S. Coskun, M. Gunoven, B. Butun, E. Ozbay, R. Turan, and H. E. Unalan, *Appl. Phys. Lett.* **103**, 083114 (2013).
- ⁹Y. Xu, C. Ni, and A. Sarangan, *Proc. SPIE* **9927**, 992707 (2016).
- ¹⁰G. Fan, H. Zhu, K. Wang, J. Wei, X. Li, Q. Shu, N. Guo, and D. Wu, *ACS Appl. Mater. Interfaces* **3**, 721 (2011).
- ¹¹S. Manna, S. Das, S. P. Mondal, R. Singha, and S. K. Ray, *J. Phys. Chem. C* **116**, 7126 (2012).
- ¹²K. Das, S. Mukherjee, S. Manna, S. K. Ray, and A. K. Raychaudhuri, *Nanoscale* **6**, 11232 (2014).
- ¹³C. Xie, P. Lv, B. Nie, J. Jie, X. Zhang, Z. Wang, P. Jiang, Z. Hu, L. Luo, Z. Zhu, L. Wang, and C. Wu, *Appl. Phys. Lett.* **99**, 133113 (2011).
- ¹⁴K.-T. Park, H.-J. Kim, M.-J. Park, J.-H. Jeong, J. Lee, D.-G. Choi, J.-H. Lee, and J.-H. Choi, *Sci. Rep.* **5**, 12093 (2015).
- ¹⁵L. Tsakalacos, J. Balch, J. Fronheiser, B. A. Korevaar, O. Sulima, and J. Rand, *Appl. Phys. Lett.* **91**, 233117 (2007).
- ¹⁶M. D. Kelzenberg, D. B. Turner-Evans, B. M. Kayes, M. A. Filler, M. C. Putnam, N. S. Lewis, and H. A. Atwater, *Nano Lett.* **8**, 710 (2008).
- ¹⁷C. Xie, J. Jie, B. Nie, T. Yan, Q. Li, P. Lv, F. Li, M. Wang, C. Wu, L. Wang, and L. Luo, *Appl. Phys. Lett.* **100**, 193103 (2012).
- ¹⁸A. K. Katiyar, S. Mukherjee, M. Zeeshan, S. K. Ray, and A. K. Raychaudhuri, *ACS Appl. Mater. Interfaces* **7**, 23445 (2015).
- ¹⁹B.-R. Huang, Y.-K. Yang, and W.-L. Yang, *Nanotechnology* **25**, 035401 (2014).
- ²⁰M.-D. Ko, T. Rim, K. Kim, M. Meyyappan, and C.-K. Baek, *Sci. Rep.* **5**, 11646 (2015).
- ²¹J. Zhu, Z. Yu, G. F. Burkhard, C.-M. Hsu, S. T. Connor, Y. Xu, Q. Wang, M. McGehee, S. Fan, and Y. Cui, *Nano Lett.* **9**, 279 (2009).

- ²²D. Li, X. Sun, H. Song, Z. Li, H. Jiang, Y. Chen, G. Miao, and B. Shen, *Appl. Phys. Lett.* **99**, 261102 (2011).
- ²³D. Lee, J. Bae, S. Hong, H. Yang, and Y.-B. Kim, *Nanotechnology* **27**, 215302 (2016).
- ²⁴Z. Huang, N. Geyer, P. Werner, J. de Boor, and U. Gösele, *Adv. Mater.* **23**, 285 (2011).
- ²⁵B. Ozdemir, M. Kulakci, R. Turan, and H. E. Unalan, *Nanotechnology* **22**, 155606 (2011).
- ²⁶J. Huang, S. Y. Chiam, H. H. Tan, S. Wang, and W. K. Chim, *Chem. Mater.* **22**, 4111 (2010).
- ²⁷A. I. Nusir and M. O. Manasreh, *IEEE Electron Device Lett.* **36**, 1172 (2015).
- ²⁸S. K. Srivastava, D. Kumar, P. K. Singh, M. Kar, V. Kumar, and M. Husain, *Sol. Energy Mater. Sol. Cells* **94**, 1506 (2010).
- ²⁹V. T. Pham, M. Dutta, H. T. Bui, and N. Fukata, *Adv. Nat. Sci.: Nanosci. Nanotechnol.* **5**, 045014 (2014).
- ³⁰O. Manasreh, *Introduction to Nanomaterials and Devices* (Wiley, Hoboken, NJ, 2012), p. 301.
- ³¹Y. Dan, K. Seo, K. Takei, J. H. Meza, A. Javey, and K. B. Crozier, *Nano Lett.* **11**, 2527 (2011).